IEEE Access
Multidisciplinary | Rapid Review | Open Access Journal

Received 21 June 2022, accepted 4 September 2022, date of publication 6 September 2022, date of current version 15 September 2022.

*Digital Object Identifier 10.1109/ACCESS.2022.3204819*

RESEARCH ARTICLE

# Analyzing Stochastic Features in Airport Surface Traffic Flow Using Cellular Automaton: Tokyo International Airport

**YOSHIAKI KAWAGOE[1], RYOHEI CHINO[1], SATORI TSUZUKI[2], ERI ITOH[3,4], AND TOMONAGA OKABE[1,5,6]**

[1]Department of Aerospace Engineering, Tohoku University, Sendai, Miyagi 980-8579, Japan
[2]Research Center for Advanced Science and Technology, The University of Tokyo, Tokyo 153-8904, Japan
[3]Department of Aeronautics and Astronautics, The University of Tokyo, Tokyo 113-8656, Japan
[4]Air Traffic Management Department, Electronic Navigation Research Institute, Chofu, Tokyo 182-0012, Japan
[5]Department of Materials Science and Engineering, University of Washington, Seattle, WA 98195, USA
[6]Research Center for Structural Materials, Polymer Matrix Hybrid Composite Materials Group, National Institute for Materials Science, Tsukuba, Ibaraki 305-0047, Japan

Corresponding author: Yoshiaki Kawagoe (kawagoe@tohoku.ac.jp)

**ABSTRACT** Global air passenger transport demand is expected to increase, and there is concern that the current airport operation will not be able to cope with aircraft overcrowding. In this study, we developed a cellular automaton (CA) simulator that can model the surface traffic of the entire Tokyo International Airport in detail, including aircraft that are arriving, taxiing, parking, and departing, using actual track data. The simulator can reproduce stop-and-go aircraft taxiing based on aircraft interactions and runway rules. It can simulate the stochastic features of the surface traffic flow. To validate the developed CA simulation, the taxiing speed distribution, local delays, and taxiing times for each route were compared with the actual track data. They were in good agreement. The effects of stochastic surface traffic features, such as arrival rate, runway occupancy time, and taxiing route, on airport operations were quantitatively analyzed. This tool could lead to a better prediction of future air traffic and improve airport operations.

**INDEX TERMS** Air-traffic management, airport surface traffic flow, cellular automaton.

## I. INTRODUCTION

The COVID-19 pandemic significantly decreased global air passenger transport demand. However, the demand is expected to return to pre-COVID-19 levels by 2024 and increase further after that [1]. Consequently, there is concern that the current air traffic control system will not be able to cope with aircraft overcrowding. Traffic congestion causes significant delays and lowers operational efficiency. They are crucial problems in airport operations with physical constraints, such as the number of runways and terminals. One solution to these problems is to expand facilities. At Tokyo International Airport in Japan, a fourth runway began operation in 2010, increasing the annual number of departures and arrivals by approximately 1.4 times [2]. However, runway and terminal expansions take several years and are expensive. Thus, they can only be applied to specific airports. Second, research has been conducted to improve the operational efficiency and throughput of airports without changing current facilities by optimizing the air traffic control system. There are three targets for optimization of airport operations: arrival, surface, and departure traffic. Especially, most aircraft behavior in surface traffic is entrusted to the pilot. Uncertainties such as aircraft separation and taxiing speed make surface traffic complex and unpredictable. In previous studies, genetic algorithms [3], [4], [5] and mixed-integer linear programming (MILP) [6] have been used to optimize taxiing routes. Additionally, a sequential surface traffic control system that advises pilots and air traffic controllers on aircraft behavior and scheduling has been proposed.

The associate editor coordinating the review of this manuscript and approving it for publication was Emre Koyuncu.

Schaper *et al.* [7] proposed the concept of time-based control of taxiing routes. It included a speed profile and coupled it with departure management. They also validated this concept through a human-in-the-loop simulation. Hayashi *et al.* [8] and Gupta *et al.* [9] proposed a spot and runway departure advisor tool. It provides guidance to air traffic controllers and airline ramp controllers for the sequencing and scheduling of push-back to improve efficiency, predictability, and throughput. Okuniek *et al.* [10] reviewed the aforementioned concepts related to air traffic optimization and clarified the contributions of the various operational parameters.

This paper focuses on Tokyo International Airport, an important airport and the busiest one in Japan. Although various optimizations have been studied as described earlier, the characteristics of surface traffic flow strongly depend on the airport. Therefore, an analysis specific to the airport is required. For the surface traffic flow at Tokyo International Airport, Chen *et al.* [11] previously developed the MILP simulator for the airport to minimize taxiing routes and time. However, the analysis does not consider the stochastic features of air traffic, such as variations in taxiing speed due to interactions between aircrafts. Moreover, it does not consider seamless aircraft behavior from landing to takeoff. Using a queuing model, Itoh *et al.* [12] suggested that stochastic features of the traffic flow, such as departure rate, taxiing time, and runway occupancy time (ROT), affect the waiting time of departure aircraft. However, the modeling of the entire airport, i.e., the connection with arrival, parking, and departure aircraft, has not been done.

In the past few decades, modeling of traffic flows using cellular automaton (CA) simulations has been conducted [13], [14], [15], [16], [17], [18]. For air traffic flow, CA simulations are widely used to optimize the alignment of arrival aircraft [19], [20]. Sekine *et al.* [21] conducted a step-back CA simulation for arrival traffic flow at Tokyo International Airport to minimize the total arrival delay and total fuel consumption. In recent years, it has been applied to surface traffic flow. Mori [22], [23] developed a CA model for Tokyo International Airport, in which the long-range interaction among aircraft is considered using a variable taxiing speed based on a floor field model. The analysis was performed for specific dates on airport layouts used before 2010. Yang *et al.* [24] analyzed surface traffic flow using a CA at Baiyun International Airport. They proposed robust off-block control strategies to reduce surface congestion. Mazur *et al.* [25] simulated surface traffic flows at Dusseldorf Airport and investigated the impact of two scenarios: a single runway closure and new runway extension. Tsuzuki *et al.* [26] conducted CA simulations for Fukuoka Airport with a junction of two taxiing routes, where particles have a volume exclusion rule to avoid collision. They revealed the relationship between throughput and route ratio. CA simulation can reproduce complex traffic flows using relatively simple rule settings. It is a useful tool that can be applied not only to ordinary operations, but also to various scenarios, such as runway closure due to an accident or expansion of airport facilities.

Table 1 summarizes the previous studies on Tokyo International Airport. To the best of our knowledge, this study is the first to develop a cellular automaton (CA) simulator that simulates the surface traffic flow over the entire area of Tokyo International Airport, that is, arrival, taxiing, parking, and departure aircraft. It can reproduce comprehensive and stochastic features of the surface traffic from landing to takeoff that have not been captured earlier. It could be used to simulate future air traffic and improve airport operation. This study modeled the surface traffic over the entire area of Tokyo International Airport and compared it with actual track data to confirm the validity of the developed simulator. In addition, initial studies were conducted to quantify the effects of arrival rate, ROT, and routes on airport operations such as taxiing time and delays.

## II. DATA ANALYSIS OF AIRPORT SURFACE TRAFFIC USING CARATS OPEN DATA

### A. DATA DESCRIPTION

First, data analysis of airport surface traffic flow at Tokyo International Airport was performed using Collaborative Actions for Renovation of Air Traffic Systems (CARATS) Open Data (COD). This is a track dataset provided by the Ministry of Land, Infrastructure, and Transport (MLIT). From the results, the features of traffic flow required for the CA simulations were obtained and used to validate the CA simulations.

The COD contains the timestamp, flight ID, latitude, longitude, altitude, and aircraft type for every second. At Tokyo International Airport, the runway configuration is selected according to the wind direction: northerly or southerly. In this study, we consider the northerly wind operation, which is the primary operation at this airport. Figure 1 shows an overview of the runway and terminal layouts at Tokyo International Airport considered here. Tokyo International Airport has four runways and three terminals. In northerly wind operations, the aircraft lands on runways 34L or 34R depending on the departure location. It takes off from runways 05 or 34R depending on the destination. Terminals 1 and 2 are for domestic flights and Terminal 3 is for international flights. Each terminal has parking spots. Each parking section of the terminal is called an "Area." For example, terminal 1 has Areas 3, 4, and 5. Area 4 has 14 parking spots. In this study, we randomly selected 20 days of northerly wind operation from 2016 to 2018 and averaged them for the data analysis. There were aircrafts parked in areas other than the eight areas mentioned earlier. However, they were excluded from this analysis because they are different from typical passenger operations, e.g., cargo and maintenance. As a result, 87.7% of all aircraft that took off and landed at Tokyo International Airport on the sampling days were included in this analysis. The arrival rate, that is, the number of arrivals per hour, was 32.78. It should be noted that the maximum arrival rate was 40 when all aircrafts were considered.

**TABLE 1. Comparison between previous studies and current study.**

| Study | Target | Model | Finding |
|---|---|---|---|
| Itoh (2020) [27] | Arrival traffic management | Queue-based model | Data analysis based on actual track data.<br>Optimal arrival strategy based on distance from arrival airport. |
| Sekine (2021) [21] | Arrival traffic management | Step-back cellular automaton | Optimal flight schedules to minimize total arrival delay and total fuel consumption. |
| Sekine (2021) [28] | Arrival traffic management | Data-driven simulation | Effects of RECAT on surrounding airspace and arrival traffic flow. |
| Hirata (2016) [29] | Runway management | Heuristic model | Sequencing strategy of arrival and departure aircrafts to improve runway capacity. |
| Itoh (2022) [12] | Runway management (Runway 05) | Time-varying fluid queue model | Estimation of waiting time in departure queue.<br>Ecological and economic benefits due to reduction in departure queue length. |
| Mori (2010) [22] | Surface traffic management (Specific date and old layout) | Cellular automaton based on Nagel-Schreckenberg model | Reproduction of surface traffic flow. |
| Mori (2013) [23] | Surface traffic management (Specific date and old layout) | Cellular automaton based on Nagel-Schreckenberg model | Reproduction of surface traffic flow.<br>Effect of weather conditions. |
| Chen (2022) [11] | Surface traffic Management (Parking was not considered) | MILP | Optimal routes to minimize taxiing routes and time.<br>Effect of reassignment of using terminals. |
| Our study | Surface traffic management (including arriving, taxiing, parking, and departing aircrafts and mutual interactions) | Cellular automaton | Data analysis based on actual track data.<br>Quantitative evaluation of traffic features (arrival rate, ROT, fluctuation, and route assignment) for airport operation. |

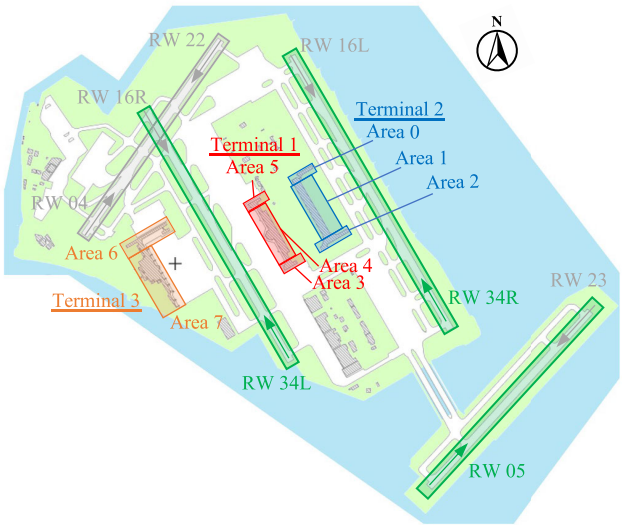


**FIGURE 1. Runway and terminal layouts at Tokyo International Airport considered in the present study [30].**

### B. SURFACE OPERATION AT TOKYO INTERNATIONAL AIRPORT

Figure 2(a) shows the tracks visualized from COD. Aircrafts coming from the north direction land at runway 34R. Those coming from the south direction land at runway 34L. The arrived aircraft moves from the runway to the parking spot via taxiing (red lines). After parking for a certain period, the aircraft is moved from the spot to the departure runway as a departure aircraft (blue lines). It took off from runway 34R in the case of a north-bound aircraft or from 05 in the case of a south-bound aircraft.

### C. USAGE RATIO OF RUNWAYS AND AREAS

Figures 3–5 show a histogram of the number of aircrafts using arrival/departure runways and parking areas for each period obtained from the COD. Here, each value is a daily average value obtained for 20 days. On the arrival runway, as shown in Fig. 3, the number of arrivals is higher from 8:00 a.m. to 11:00 p.m., where domestic and Asian flights are active. Runway 34L is primarily used because runway 34R is also used as a departure runway. Conversely, only runway 34R is used in the late-night period as it is used for European and U.S. flights. For the departure runways (Fig. 4), runway 05 is primarily used for the departure runway. The number of departures increased from 6:00 a.m. to 9:00 p.m. The area usage ratios are shown in Fig. 5. The ratios of domestic areas, especially in Areas 1 and 4 with many parking spots, are large from 6:00 a.m. to 11:00 p.m. During this time, there are many take-offs and landings, as mentioned above. Contrarily, only Areas 6 and 7 for international flights were used during the late night period.

### D. TAXIING SPEED

Next, taxiing speeds were calculated from the time and location information of each aircraft in the COD. Their distribution is shown in Fig. 6. This is the average value during the peak hours from 8:00 a.m. to 9:00 p.m. Figure 6(a) shows the overall view, and (b) and (c) show the enlarged views around the runways. From the distributions, the taxiing speeds were 10∼20 kt on the normal taxiing routes, 20∼30 kt on the high-speed sections (e.g., the straight ways from runway 34R to Terminal 3), less than 5 kt around the spots, and more than 120 kt on the runways. There were localized low-speed regions in front of departure runways 05 and 34R. This is because aircrafts that cannot enter the runway due to ROT form a departure queue. It is disadvantageous from the viewpoint of fuel saving as they are waiting while idling. Itoh *et al.* [12] reported a similar taxiing speed distribution and queues around runways at Tokyo International Airport.

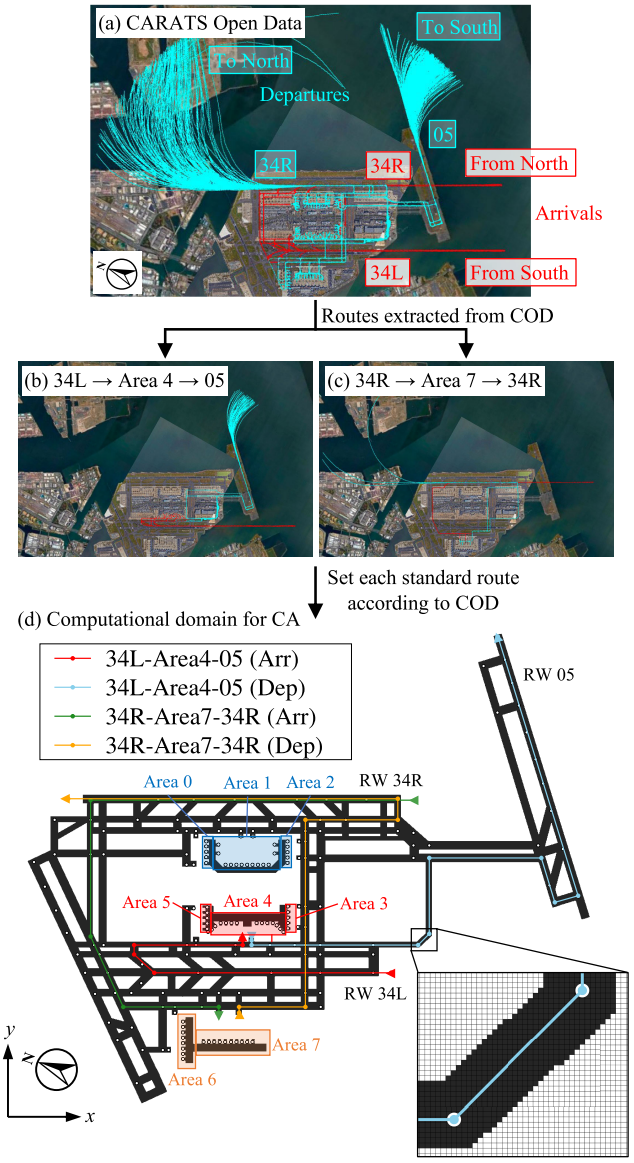


**FIGURE 2.** Schematic of obtaining standard route from COD for CA simulations: (a) track visualization from COD, (b) and (c) extracted particular routes, and (d) computational domain for CA simulation and examples of standard routes.

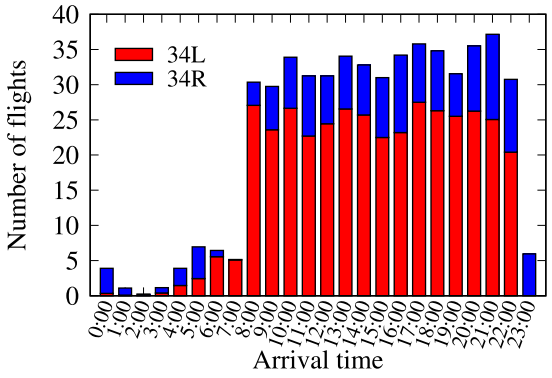


**FIGURE 3.** Histogram of the number of aircrafts using arrival runways in a day obtained from COD.

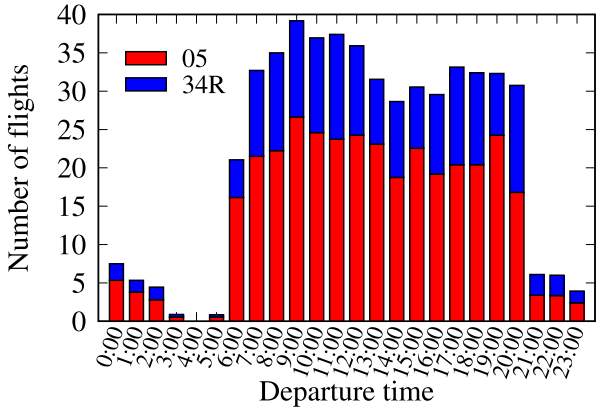


**FIGURE 4.** Histogram of the number of aircrafts using departure runways in a day obtained from COD.

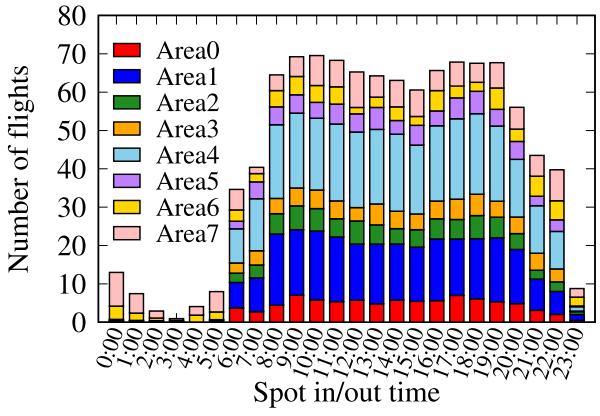


**FIGURE 5.** Histogram of the number of aircrafts using areas in a day obtained from COD.

They developed a time-varying fluid queue model for the departure queue at runway 05 and evaluated the ecological and economic benefits of a reduction in the departure queue length.

In addition, arrivals and departures using Terminal 3 need to cross 34L. However, they are not allowed to do so when runway 34L is in use or approached by arrivals. This also creates localized low-speed regions at the intersection with runway 34L. These local delays are important features that limit efficient operation and fuel savings.

### *E. IDENTIFICATION OF AIRCRAFT ROUTES*

The COD assigns different flight IDs for arrival and departure aircrafts. Thus, even if they are the same aircraft, it is impossible to directly determine the route from landing to takeoff. Two methods were used to obtain the features of the aircraft routes. The first is a probabilistic method. The usage ratio of each route can be calculated by multiplying the arrival runway usage ratio, $P_{\mathrm{arr}}$, area usage ratio from each arrival runway, $P_{\mathrm{arr-area}}$, and departure runway usage ratio from each area, $P_{\mathrm{area-dep}}$, using the following equation:

$$P_{\mathrm{route}} = P_{\mathrm{arr}} \times P_{\mathrm{arr-area}} \times P_{\mathrm{area-dep}}. \quad (1)$$

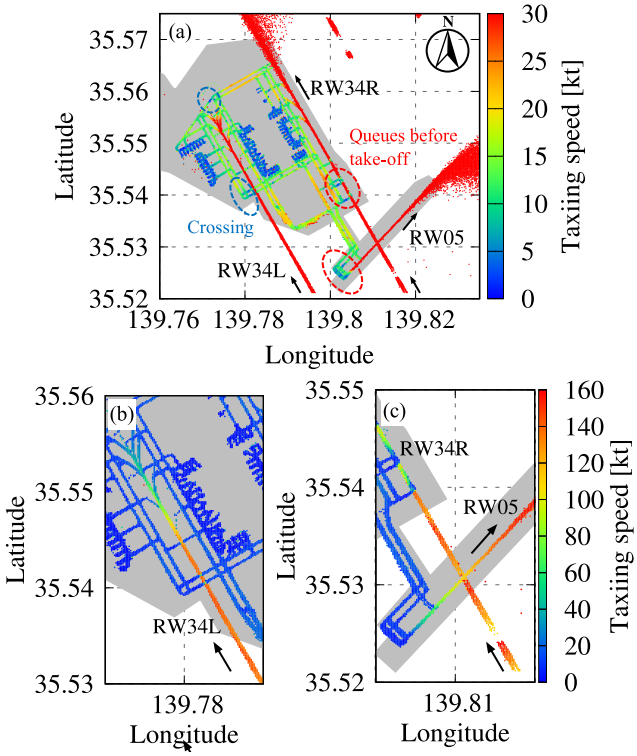


**FIGURE 6.** Taxiing speed distributions obtained in COD: (a) overall view and (b)(c) enlarged views around runways.

**TABLE 2.** Usage ratio, $P_{arr}$, of arrival runway.

| Arrival runway | Usage ratio |
|---|---|
| 34L | 0.7695 |
| 34R | 0.2305 |

These usage ratios were calculated from the COD during peak hours. Tables 1–3 show the values of $P_{arr}$, $P_{arr-area}$, and $P_{area-dep}$. Fig 7 shows a comparison of the usage ratios for each route obtained using (1). For example, the usage ratio of 34L→ Area 1→05 can be calculated as

$$\begin{aligned} P_{34L-Area1-05} &= P_{34L} \times P_{34L-Area1} \times P_{Area1-05} \\ &= 0.7695 \times 0.2160 \times 0.6773 \\ &= 0.1125. \end{aligned} \tag{2}$$

For Terminal 2, 34L→Area 1→05 was the primary route. However, other routes were also used relatively frequently. For Terminal 1, the ratio 34L→Area 4→05 is used much more frequently than that for the other routes. For Terminal 3, the route landing at runway 34L was approximately five times more frequently used than the route landing at runway 34R. This might be due to the proximity of the runway to the terminal and to avoid crossing the runway 34L.

In the second method, when the arrival and departure aircraft of the same aircraft type consecutively used the same parking spot, the two aircraft were considered to be the same aircraft. The standard routes from landing to takeoff and parking times were estimated using the track data of the two aircraft. Aircrafts that did not meet the aforementioned rules were excluded. 45.7% of the total aircrafts were used for route

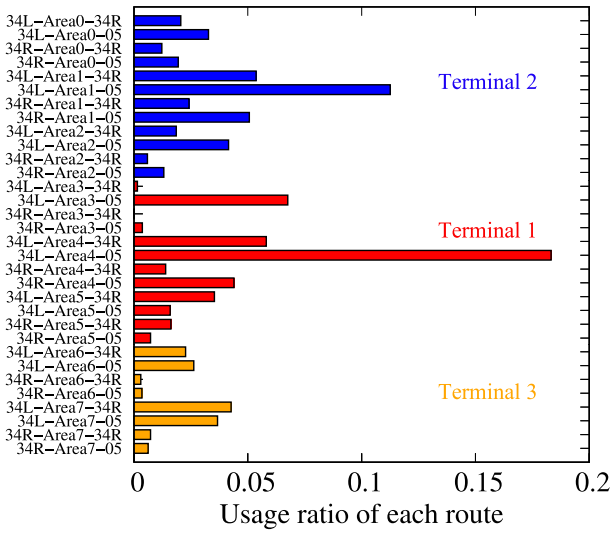


**FIGURE 7.** Usage ratios of respective routes calculated from (1).

**TABLE 3.** Usage ratio, $P_{arr-area}$, of areas from respective arrival runways.

| Runway–Area | Usage ratio | Runway–Area | Usage ratio |
|---|---|---|---|
| 34L–Area0 | 0.0692 | 34R–Area0 | 0.1374 |
| 34L–Area1 | 0.2160 | 34R–Area1 | 0.3247 |
| 34L–Area2 | 0.0781 | 34R–Area2 | 0.0824 |
| 34L–Area3 | 0.0898 | 34R–Area3 | 0.0163 |
| 34L–Area4 | 0.3136 | 34R–Area4 | 0.2509 |
| 34L–Area5 | 0.0666 | 34R–Area5 | 0.1018 |
| 34L–Area6 | 0.0636 | 34R–Area6 | 0.0280 |
| 34L–Area7 | 0.1031 | 34R–Area7 | 0.0585 |

identification. In the northerly wind operation, two arrival runways, eight areas, and two departure runways were considered. Thus, 32 standard routes were identified. Figure 2(b) and (c) show a particular route, for example, 34R→Area 7→34R is a route along the outer edge of the airport. Parking time was calculated from the difference between the spot-in and spot-out times of the same aircraft. The mode frequencies of parking time were calculated separately for domestic and international terminals. The mode frequencies were 2700 and 5700 s, respectively. This result is in agreement with previous studies [31].

## III. AIRPORT SURFACE TRAFFIC SIMULATION USING CELLULAR AUTOMATON

In this study, CA simulation on a two-dimensional lattice model proposed by Tsuzuki *et al.* [26] was used to reproduce the airport surface traffic flow at Tokyo International Airport. In this section, a basic description of the CA and the newly implemented velocity-setting method and runway rules are presented.

### A. BASIC RULE OF CELLULAR AUTOMATON

Figure 2(d) shows the computational domain of the CA simulations. This computational domain is an extension of the one proposed in [32]. The two-dimensional domain was divided into 1408 × 1126 cells in the $x$ and $y$ directions

**TABLE 4.** Usage ratio, $P_{\text{area-dep}}$, of departure runways from respective areas.

| Area–Runway | Usage ratio | Area–Runway | Usage ratio |
|---|---|---|---|
| Area0–05 | 0.6146 | Area4–05 | 0.7592 |
| Area0–34R | 0.3854 | Area4–34R | 0.2408 |
| Area1–05 | 0.6773 | Area5–05 | 0.3105 |
| Area1–34R | 0.3227 | Area5–34R | 0.6895 |
| Area2–05 | 0.6909 | Area6–05 | 0.5372 |
| Area2–34R | 0.3091 | Area6–34R | 0.4628 |
| Area3–05 | 0.978 | Area7–05 | 0.4623 |
| Area3–34R | 0.022 | Area7–34R | 0.5377 |

(1 cell = 4.73 m). As shown in the inset in Fig. 2(d), the black cells represent the runways and taxiways. The cells selected from the black cells are the white points in Fig. 2(d) called ''checkpoints'' to construct aircraft routes. As mentioned in section II-E, 32 standard routes were obtained from the COD. Each route was defined in the computational domain using checkpoints, as shown in Fig. 2(d). Figure 8 shows the schematic of the proposed CA model. Particles modeling an aircraft travel along a route defined by checkpoints. Now, we consider a particle moving from checkpoints A to B (Fig. 8(a)–(c)). The particle travels with a velocity vector for each step. The position of the particle on the cell is then determined by integerizing the updated coordinates. The direction of the velocity vector was updated at every step in the direction from the particle's current position to the next checkpoint. This allows the particle to travel discretely along an arbitrary route defined by the two checkpoints. In this simulation, the time step was set to 1 s.

Particles have exclusion spaces, called ''antennas,'' for collision detection in the front and back (Fig. 8(d)). When the antennas contact each other in the same lane or cross each other at an intersection, one of the particles is instructed to stop. Thus, collision between particles is avoided. There is no strict rule for the distance between the aircraft on the ground. However, in this study, antennas with a length of 24 cells (= 113.52 m) were installed at the front and rear. For this antenna length, the minimum separation between aircrafts is approximately one aircraft size when the antennas cross each other. See [26] for details on the priority and pattern of stop instructions.

### B. STOCHASTIC VELOCITY SETTING ON CA

Typical CA models cannot use arbitrary velocities as the particle coordinates are defined in the cell. In other words, a taxiing speed of 2.4 cells/step was not possible. Therefore, in a typical CA simulation, the traveling speed is strongly dependent on the definition of cell size [23]. If the number of cells representing the region is significant, fine-speed settings would be possible. However, this would be very time-consuming and computationally expensive. Therefore, in this study, we used a method that could reproduce arbitrary speeds stochastically in the CA model.

For example, the taxiing speed $v_{\text{tx}}$ is set to 22 kt (= 2.4 cells/s). We generate a uniform random number, $a$, at every step and stochastically round the setting speed using the fractional part of the setting speed, 0.4, as follows:

$$v_{\text{tx}} = \begin{cases} 2 & \text{if } a > 0.4 \\ 3 & \text{if } a < 0.4. \end{cases} \tag{3}$$

The taxiing speed in this step was $v_{\text{tx}} = 2$ or 3. By repeating this process, the taxiing speed becomes 2.4 cells/s, which is an arbitrary particle speed. Figure 9 shows the results of the verification of the aforementioned procedure on runway 34L. The horizontal and vertical axes represent the setting speed and actual particle speed calculated from the time required for the move. The actual speed reproduced the setting speed well, confirming the validity of the speed determination method.

In the present simulations, the taxiing speed $v_{\text{tx}}$ was set as follows according to Fig. 6:

$$v_{\text{tx}} = \begin{cases} 5 \text{ kt} & \text{in area} \\ 14 \text{ kt} & \text{in normal taxiing way} \\ 20 \text{ kt} & \text{in high speed section} \\ 140 \text{ kt} & \text{in runway.} \end{cases} \tag{4}$$

### C. RUNWAY RULES

#### 1) RUNWAY OCCUPANCY TIME (ROT)

ROT is an important factor in determining airport performance. It is the buffer time for safe take-offs and landings. Accurate prediction and optimization of the ROT can improve take-off/landing throughput [12], [28], [33], [34]. In a previous study of Tokyo International Airport, the ROT was set at 95 s for consecutive takeoff and 115 s for consecutive landing from the entry of the preceding aircraft onto the runway [29]. In this CA simulation, it took approximately 40–50 s from entry to exit on the runway. Therefore, an additional buffer time of 80 s was set for the total ROT of approximately 120–130 s. This value is reasonable compared to the actual data (approximately 130 s) at runway 05 [12]. For simplicity, the same ROT was used for all takeoff and landing combinations.

#### 2) LANDING CLEARANCE

Once a landing clearance has been issued, no other aircraft can take off, land, or cross on the runway. To model the runway constraints, this study assumes that the landing clearance should be issued before reaching 1 NM from the runway arrival threshold [29]. Assuming that the flight speed in the final approach is the same as $v_{\text{tx}}$ on the runway, the time required to fly 1 NM is 1 NM/140 kt $\simeq$ 26 s. In the present CA simulation, particles enter at the end of the runway and remain there for 26 s. This represents the final approach of an approaching aircraft that has received landing clearance. During this time, no other aircraft can use or cross the runway.

### D. SIMULATION PROCEDURE

Finally, the simulation procedure is described. A time table containing arrival times, routes (arrival and departure runways, and areas), and parking times for each aircraft was determined based on the usage ratio in Section II-E. Here,

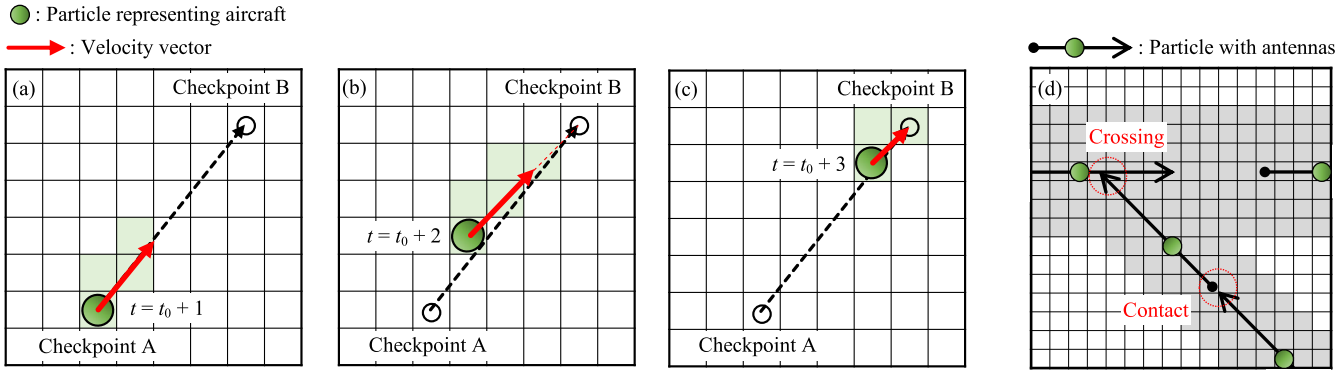


**FIGURE 8.** Schematic of (a)–(c) particle movement and (d) antenna in the present CA model.

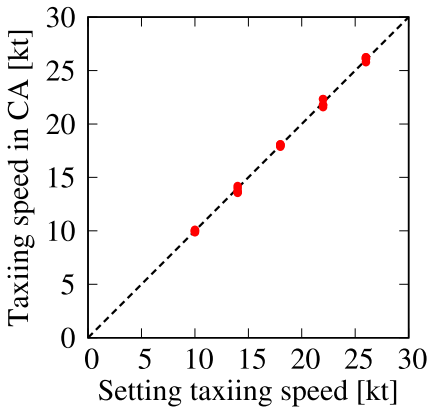


**FIGURE 9.** Comparison of taxiing speed determined using stochastic rounding with setting values.

the scheduled arrival rate $\lambda_{arr}$ was set to 33, according to the COD results. Thus, on runway 34L, which is used only for landing, an arrival aircraft is scheduled every 141 s ($= 3600/(\lambda_{arr} \cdot P_{34L})$). On runway 34R, which is used for takeoff and landing, an arriving aircraft is scheduled at the same interval for runway 34L and only when $a > P_{34R}/P_{34L}$. Here, $a$ is a random number. The resulting arrival rate at runway 34R is $\lambda_{arr} \cdot P_{34R}$. Based on the time table, if the arrival runway is available, particles are injected into the arrival runway as an approaching aircraft 26 s before the arrival time. If it is not available due to takeoff of other aircraft or ROT, the arrival time is delayed by 1 s. The entered particles pass through the following four statuses:

APP: Approaching aircraft. The aircraft enters the end of the arrival runway and remains there for 26 s. While it remains there, other aircrafts cannot take off, land, or cross this runway according to the landing clearance rule.

ARR: Arrival aircraft. After a 26 s stay, the aircraft begins landing and taxiing to the spot. At a checkpoint immediately before the area, the aircraft randomly selects a parking spot from available spots in the area. If there is no available spot, the aircraft waits at this checkpoint until a spot opens.

PRK: Parking aircraft. The aircraft are stopped for a specified parking time at the parking spot. The parking times are 2700 and 5700 s for the domestic and international terminals, respectively.

DEP: Departure aircraft. After the aircraft is parked, it begins taxiing from the spot to the departure runway and takes off. When the aircraft reaches the checkpoint at the end of the runway, it is removed from the simulation domain. The takeoff time is recorded.

During one step, (a) collision detection by the antenna, (b) application of the runway rules, (c) stop instruction, and (d) updating of coordinates were performed in this order. We set the physical time and total number of time steps to be 1 s and 180,000, respectively. It corresponds to 50 h, in which arrivals and departures are repeated to ensure sufficient statistics. Each feature was sampled in a steady state, i.e., in 40 h excluding the beginning and last five hours. Three calculations were performed under the same operator conditions with different time tables. The average value was calculated.

## IV. RESULTS AND DISCUSSION

### A. VALIDATION OF CA SIMULATION

The first step was to verify the validity of the CA simulation by comparing it with the COD. Figure 10 presents a snapshot of the CA simulation. Note that multiple snapshots were combined and illustrated for the reader's clear understanding. Each particle was colored according to its status. Queues of several aircrafts were generated in front of departure runways 05 and 34R caused by the ROT. The departing aircraft could not cross runway 34L and was stopped because the approaching aircraft (APP) was standing on runway 34L.

Figure 11 shows the taxing speed distribution obtained from the CA simulation. As described in Section III-B, four taxiing speeds were set in the CA simulation. However, there were several areas where interactions with other aircrafts reduced the speed, causing delays. The first is the blue region in front of the departure runway, which corresponds to the queue before takeoff. The second is the blue region (shown

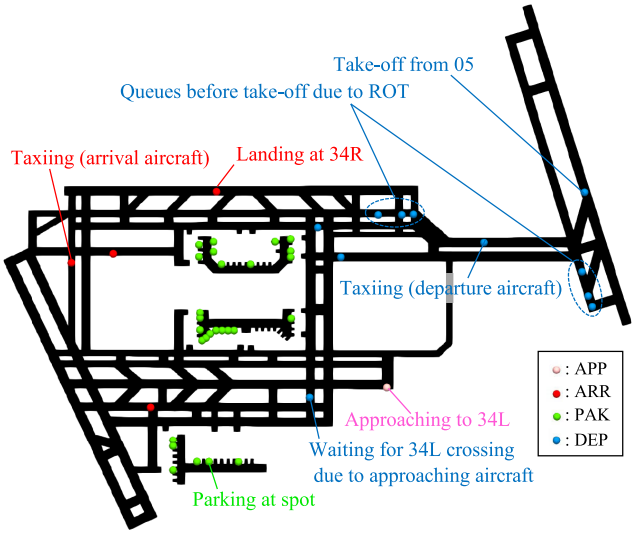


**FIGURE 10.** Snapshot of the CA simulation.

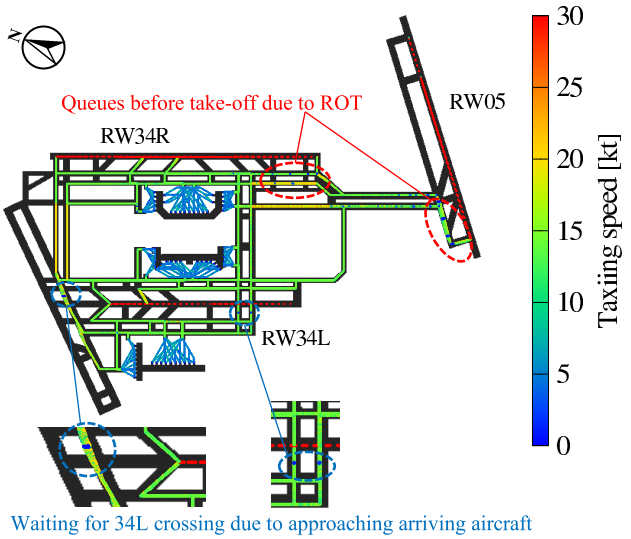


**FIGURE 11.** Taxiing speed distribution in the CA simulations.

enlarged) of taxiing ways intersecting runway 34L, which indicates that the delay is due to a stop instruction based on the rules of the landing clearance. These characteristics of the taxiing speed distribution are in good agreement with those in Fig. 6 obtained from the COD. The CA simulation reproduces the localized delays caused by aircraft interactions and runway rules.

Figure 12 compares the average taxiing times for each route obtained in the CA simulation with those obtained in the COD. Here, we discuss them separately for arrival and departure aircraft. The taxiing times of departures tend to be longer than those of arrivals, even though the actual lengths of the routes are approximately equal. This is due to the queue of departures before takeoff, as mentioned earlier. It delays all departure routes. The taxiing time in the CA simulation reproduces the taxiing time in the COD well, especially capturing the trend of each route and tendency of the taxiing time to increase for departures.

Consequently, the present CA simulation reproduced the surface traffic flow of Tokyo International Airport well. It was a valid tool for investigating the optimal operation of the airport.

### *B. ANALYSIS FOR VARIOUS OPERATIONAL PARAMETERS*

In this section, we quantitatively evaluate the effects of surface traffic features on airport operations using the CA simulations.

#### 1) ARRIVAL RATE

The arrival rate is the number of landing aircrafts per hour and is the most fundamental operational parameter. Here, the scheduled arrival rate $\lambda_{\mathrm{arr}}$ was varied from 30 to 35, whereas the usage ratio remained the same. Figure 13 shows the relationship between the arrival and departure throughputs for each runway and scheduled arrival rate. Throughput indicates the actual number of take-offs and landings per hour and is one of the indicators of airport performance. The red and blue bars represent the arrival throughput using runways 34L and 34R, respectively. The green and orange bars represent the departure throughput using runways 05 and 34R, respectively. As $\lambda_{\mathrm{arr}}$ increases, the throughput increases by the same amount, indicating that take-offs and landing at the airport occur without problems as scheduled. As mentioned earlier, the actual max arrival rate was 40. Thus, this result is reasonable because this analysis is within the actual runway allowance. Figure 14 shows the delays in arrival and departure taxiing as functions of $\lambda_{\mathrm{arr}}$. Here, delay is defined as the increment from the taxiing time, $T_{\mathrm{tx,min}}$, when the aircraft travels without interactions with other aircraft, that is, without delay. The delays on arrival and departure taxiing are denoted as $T_{\mathrm{d,arr}}$ and $T_{\mathrm{d,dep}}$, respectively. These delays include stops to avoid collisions with other aircraft, stops before runways owing to ROT and queues, and stops prior to runway crossings. In arrival taxiing, there is approximately zero delay, regardless of the arrival rate. However, in the case of departure taxiing, the delay increases as the scheduled arrival rate increases. Figure 15 shows the taxiing speed distribution around runway 05 when the arrival rates are 30 and 35, respectively. The queue of departures is longer when the arrival rate is 35. This queue causes a departure waiting time, resulting in increased delays in departure taxiing. For optimal airport operation, it is necessary to achieve a high throughput and low delay. This result suggests that an increase in the arrival rate increases the throughput and local delay. Thus, the departure schedule such as off-block time needs to be optimized to remove the queues.

#### 2) ROT

The ROT limits the entry of a departure aircraft onto the runway, creating queues for departure aircrafts. Optimizing the ROT within the range of safe take-offs and landings is one way to improve the airport performance. Here, we evaluated

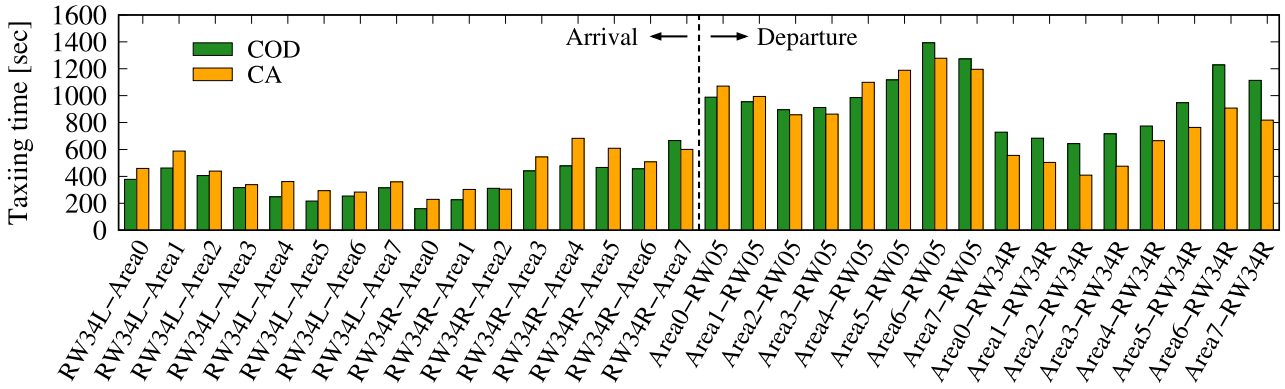


**FIGURE 12.** Comparison of taxiing time for each route obtained in the CA simulation with COD.

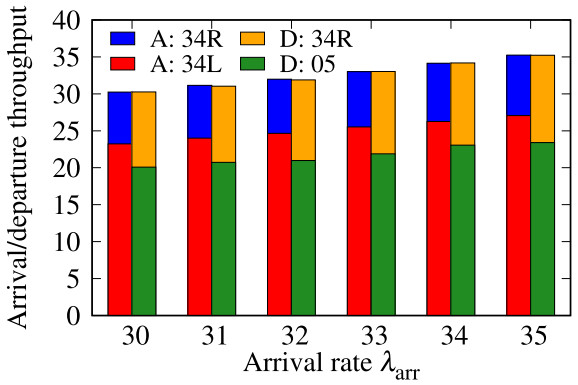


**FIGURE 13.** Throughput of arrival/departure runways for various scheduled arrival rates $\lambda_{arr}$.

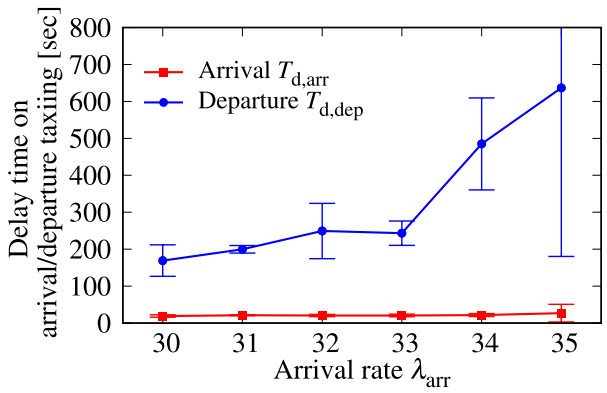


**FIGURE 14.** Delay times on arrival/departure taxiing as functions of arrival rate $\lambda_{arr}$.

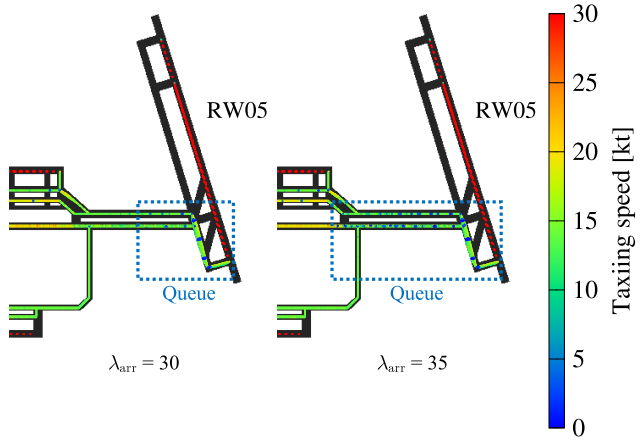


**FIGURE 15.** Taxiing speed distribution around runway 05 for arrival rates of 30 and 35.

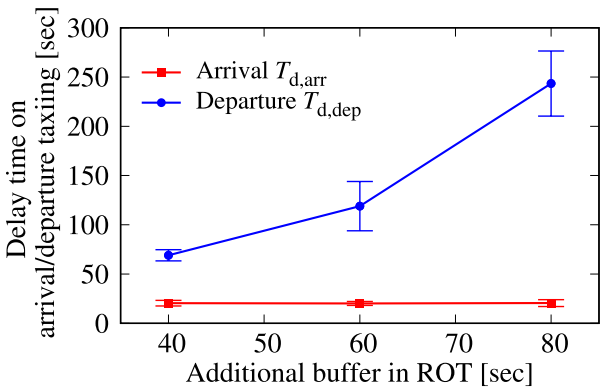


**FIGURE 16.** Delay times on arrival/departure taxiing as functions of additional buffer time in ROT.

the delay when the additional buffer in the ROT was reduced to 80, 60, and 40 s. The arrival rate was 33, and the usage ratio was the same. Decreasing the additional buffer from 80 to 40 s significantly reduced the delay in departure from 243 to 69 s (Fig. 16). This is because the succeeding aircraft in the queue is redundantly affected by the delayed preceding aircraft owing to ROT. Consequently, the elimination or shortening of the queue reduces the departure waiting time by more than the reduction in ROT (40 s). This suggests that ROT optimization is highly effective in improving airport performance.

### 3) FLUCTUATION OF ARRIVAL INTERVAL

Itoh *et al.* [27] analyzed the traffic flow of aircraft arriving at Tokyo International Airport using a queue-based model to identify the optimal arrival strategy based on the distance from the arrival airport. They showed that fluctuations in flight time and arrival rate at each flight area are important parameters in determining the delay. Therefore, in this study, we evaluate the effect of fluctuations in the arrival interval

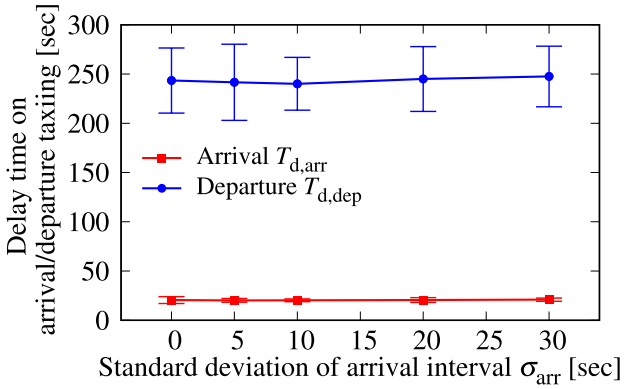


**FIGURE 17.** Delay times of arrival/departure taxiing as functions of standard deviation $\sigma_{arr}$ of arrival interval.

time on surface traffic flow. The value of the fluctuations was randomly selected from a Gaussian distribution with a mean of 0 s and a standard deviation of $\sigma_{arr}$. The arrival time is updated by adding the fluctuation value. Therefore, the updated arrival intervals at runway 34L were based on a Gaussian distribution with a mean of 141 s and a standard deviation of $\sigma_{arr}$.

Figure 17 shows taxiing delays as a function of the standard deviation of the arrival interval $\sigma_{arr}$. The arrival and departure taxiing delays change negligibly even as $\sigma_{arr}$ increases. At the current arrival rate, the effect of the fluctuation of several tens of seconds is masked by the effects of the ROT and other factors. However, under an overcrowded take-off/landing schedule with a high arrival rate, the effect of the fluctuation is expected to be significant.

#### 4) ROUTE RE-ASSIGNMENT

Chen *et al.* [11] used MILP to optimize airport surface operations at Tokyo International Airport and re-assign aircraft routes. Specifically, the domestic terminal was changed (Terminal 1 → 2 or Terminal 2 → 1) for aircrafts that choose a route where the runways were far from the terminal due to the terminal-airline restrictions. This is impractical because the aircrafts parked at a terminal are controlled by different airlines. However, this reassignment decreased taxiing distance and time. This analysis did not consider arrival and departure aircraft connections or spot occupancy. Thus, it is mentioned that the effect might be overestimated. In the present study, the effect of route reassignment was examined based on the same strategy. In this CA simulation, the arrival, parking, and departure taxiing were analyzed in series using the same particles, allowing the effects to be verified more accurately. The terminals on the six long-distance routes were changed as shown in Table 5. For example, in route 34L→Area 1→05, Area 1 (Terminal 2) is far from runway 34L. Thus, the parking area is changed to Area 4 (Terminal 1), which is closer to runway 34L. This reduces $T_{tx,min}$ for most of the routes. The CA simulation reproduced this route reassignment by changing the usage ratio of the routes. Denoting the ratio of terminal exchanges as $\alpha$, the respective usage ratios

**TABLE 5.** Route re-assignment and $T_{tx,min}$ of each route.

| Original route ($T_{tx,min}$) | | Re-assigned route ($T_{tx,min}$) |
|---|---|---|
| 34L-Area0-05 (1112 sec) | → | 34L-Area5-05 (1154 sec) |
| 34L-Area1-05 (1261 sec) | → | 34L-Area4-05 (1086 sec) |
| 34L-Area2-05 (965 sec) | → | 34L-Area3-05 (886 sec) |
| 34R-Area3-05 (1124 sec) | → | 34R-Area2-05 (776 sec) |
| 34R-Area4-05 (1422 sec) | → | 34R-Area1-05 (977 sec) |
| 34R-Area5-05 (1485 sec) | → | 34R-Area0-05 (953 sec) |

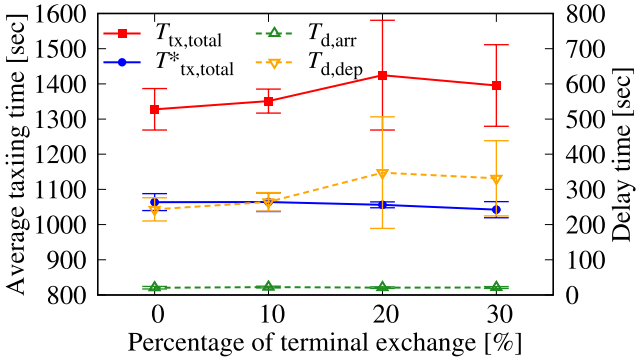


**FIGURE 18.** Average total taxiing times and delay times on arrival/departure taxiing as functions of terminal exchange ratio.

are given as follows:

$$P'_{34L-Area1-05} = P_{34L-Area1-05} - \alpha P_{34L-Area1-05} \quad (5)$$

$$P'_{34L-Area4-05} = P_{34L-Area4-05} + \alpha P_{34L-Area1-05} \quad (6)$$

Figure 18 shows the total taxiing times and delay times as functions of terminal exchange ratio $\alpha$. Here, $T_{tx,total}$ is the average of the sum of arrival/departure taxiing times among all sampling aircrafts. $T^*_{tx,total}$ is the value from which delays are excluded, $T^*_{tx,total} = T_{tx,total} - T_{d,arr} - T_{d,dep}$. As $\alpha$ increases, $T^*_{tx,total}$ decreases. It indicates that the taxiing time excluding delays decreases owing to route reassignment. However, as $T^*_{tx,total}$ decreases, the departure interval becomes smaller. Thus, a queue before the departure runway is more likely to form. Consequently, the departure taxiing delay increases with $\alpha$. $T_{tx,total}$ changes negligibly regardless of $\alpha$. Similar to the results for the arrival rate mentioned earlier, this problem could be solved by optimizing the departure schedule. Spot utilization beyond the terminal-airline restriction could become an important factor in optimizing airport operations.

## V. CONCLUSION

In this study, CARATS Open Data (COD), which is actual track data, was analyzed to reveal the surface traffic features at the Tokyo International Airport. Using the features—arrival rates, routes, taxiing speeds, and usage ratios—obtained from the COD, a cellular automaton (CA) simulation was developed to reproduce the complex surface traffic flow over the entire area of Tokyo International Airport. To validate the CA simulation, the taxiing speed distribution, local delays before runways, and taxiing times for each route were compared with the COD. They were in good agreement.

In reality, it is difficult to evaluate the effects of varying various operational parameters at an operational airport. As an initial study, the effects of surface traffic features—arrival rate, runway occupancy time (ROT), fluctuation of arrival interval, and route re-assignment—on airport operations, such as the taxiing time and delays, were quantitatively evaluated. The developed CA simulation provides an important guide for developing optimization strategies for airport operations. Furthermore, CA simulations could predict the effects of layout changes, new routes, and new facility expansion, which are difficult to evaluate in reality. They can contribute not only to operational optimization but also to airport expansion planning.

## ACKNOWLEDGMENT

The visualization of CARATS open data in Figure 2 uses Gaia Viewer developed by Prof. Yasufuku (Osaka University). Special thanks go to Prof. Yasufuku for providing technical support.

## REFERENCES

[1] International Air Transport Association. *Five Years to Return to the Pre-Pandemic Level of Passenger Demand*. Accessed: Apr. 18, 2022. [Online]. Available: https://www.iata.org/en/iata-repository/publications/economic-reports/Five-years-to-return-to-the-pre-pandemic-level-of-passenger-demand/

[2] Ministry of Land. Infrastructure and Transport. *MLIT: Aircraft Movement (Japanese)*. Accessed: Apr. 18, 2022. [Online]. Available: https://www.mlit.go.jp/koku/15_bf_000185.html

[3] B. Pesic, N. Durand, and J.-M. Alliot, "Aircraft ground traffic optimisation using a genetic algorithm," in *Proc. Genetic Evol. Comput. Conf.*, 2001, pp. 1397–1404.

[4] J.-B. Gotteland and N. Durand, "Genetic algorithms applied to airport ground traffic optimization," in *Proc. Congr. Evol. Comput. (CEC)*, 2003, pp. 544–551.

[5] C. Liu and K. Guo, "Airport taxi scheduling optimization based on genetic algorithm," in *Proc. Int. Conf. Comput. Intell. Secur.*, Dec. 2010, pp. 205–208.

[6] J. W. Smeltink, M. J. Soomer, P. de Waal, and R. van der Mei, "An optimisation model for airport taxi scheduling," in *Proc. INFORMS Annu. Meeting*, Oct. 2004. [Online]. Available: http://citeseerx.ist.psu.edu/viewdoc/summary?doi=10.1.1.116.9774

[7] M. Schaper and I. Gerdes, "Trajectory based ground movements and their coordination with departure management," in *Proc. IEEE/AIAA 32nd Digit. Avionics Syst. Conf. (DASC)*, Oct. 2013, pp. 1B4-1–1B4-9.

[8] M. Hayashi, T. Hoang, Y. C. Jung, W. Malik, H. Lee, and V. L. Dulchinos, "Evaluation of pushback decision-support tool concept for charlotte Douglas international airport ramp operations," in *Proc. 11th USA/Eur. Air Traffic Manag. Res. Develop. Seminar (ATM)*, 2015, pp. 1–10.

[9] G. Gupta, W. Malik, L. Tobias, Y. Jung, T. Hoang, and M. Hayashi, "Performance evaluation of individual aircraft based advisory concept for surface management," in *Proc. 10th USA/Eur. Air Traffic Manag. Res. Develop. Seminar, (ATM)*, 2013, pp. 1–11.

[10] J. N. Okuniek, I. Gerdes, J. Jakobi, T. Ludwig, B. L. Hooey, D. Foyle, Y. C. Jung, and Z. Zhu, "A concept of operations for trajectory-based taxi operations," in *Proc. 16th AIAA Aviation Technol., Integr., Oper. Conf.*, Jun. 2016, p. 3753.

[11] T. Chen and S. Hanaoka, "Improvement of airport surface operation at Tokyo international airport using optimization approach," *Aerospace*, vol. 9, no. 3, p. 145, Mar. 2022.

[12] E. Itoh, M. Mitici, and M. Schultz, "Modeling aircraft departure at a runway using a time-varying fluid queue," *Aerospace*, vol. 9, no. 3, p. 119, Feb. 2022.

[13] K. Nagel and M. Schreckenberg, "A cellular automaton model for freeway traffic," *J. Phys. De I*, vol. 2, pp. 2221–2229, Dec. 1992, doi: 10.1051/jp1:1992277.

[14] J. Esser and M. Schreckenberg, "Microscopic simulation of urban traffic based on cellular automata," *Int. J. Modern Phys. C*, vol. 8, no. 5, pp. 1025–1036, Oct. 1997.

[15] H. Ito and K. Nishinari, "Totally asymmetric simple exclusion process with a time-dependent boundary: Interaction between vehicles and pedestrians at intersections," *Phys. Rev. E, Stat. Phys. Plasmas Fluids Relat. Interdiscip. Top.*, vol. 89, no. 4, Apr. 2014, Art. no. 042813. [Online]. Available: https://journals.aps.org/pre/abstract/10.1103/PhysRevE.89.042813

[16] H. Yamamoto, D. Yanagisawa, and K. Nishinari, "Velocity control for improving flow through a bottleneck," *J. Stat. Mech., Theory Exp.*, vol. 2017, no. 4, Apr. 2017, Art. no. 043204. [Online]. Available: https://iopscience.iop.org/article/10.1088/1742-5468/aa5a73

[17] S. Tsuzuki, D. Yanagisawa, and K. Nishinari, "Effect of self-deflection on a totally asymmetric simple exclusion process with functions of site assignments," *Phys. Rev. E, Stat. Phys. Plasmas Fluids Relat. Interdiscip. Top.*, vol. 97, no. 4, pp. 4–6, Apr. 2018.

[18] S. Tsuzuki, D. Yanagisawa, and K. Nishinari, "Effect of walking distance on a queuing system of a totally asymmetric simple exclusion process equipped with functions of site assignments," *Phys. Rev. E, Stat. Phys. Plasmas Fluids Relat. Interdiscip. Top.*, vol. 98, no. 4, pp. 4–6, Oct. 2018.

[19] W.-X. Lim and Z.-W. Zhong, "Re-planning of flight routes avoiding convective weather and the 'Three Area,'" *IEEE Trans. Intell. Transp. Syst.*, vol. 19, no. 3, pp. 868–877, Mar. 2018.

[20] S.-J. Wang and Y.-H. Gong, "Research on air route network nodes optimization with avoiding the three areas," *Saf. Sci.*, vol. 66, pp. 9–18, Jul. 2014.

[21] K. Sekine, T. Tatsukawa, E. Itoh, and K. Fujii, "Multi-objective take-off time optimization using cellular automaton-based simulator," *IEEE Access*, vol. 9, pp. 79461–79476, 2021.

[22] R. Mori, "Modeling of aircraft surface traffic flow at congested airport using cellular automata," in *Proc. 4th Int. Conf. Res. Air Transp.*, 2010, pp. 1–6.

[23] R. Mori, "Aircraft ground-taxiing model for congested airport using cellular automata," *IEEE Trans. Intell. Transp. Syst.*, vol. 14, no. 1, pp. 180–188, Mar. 2013.

[24] L. Yang, S. Yin, K. Han, J. Haddad, and M. Hu, "Fundamental diagrams of airport surface traffic: Models and applications," *Transp. Res. B, Methodol.*, vol. 106, pp. 29–51, Dec. 2017.

[25] F. Mazur and M. Schreckenberg, "Simulation and optimization of ground traffic on airports using cellular automata," *Collective Dyn.*, vol. 3, pp. 1–22, Mar. 2018.

[26] S. Tsuzuki, D. Yanagisawa, and K. Nishinari, "Throughput reduction on an air-ground transport system by the simultaneous effect of multiple traveling routes equipped with parking sites," *J. Phys. Commun.*, vol. 4, no. 5, May 2020, Art. no. 055009.

[27] E. Itoh and M. Mitici, "Evaluating the impact of new aircraft separation minima on available airspace capacity and arrival time delay," *Aeronaut. J.*, vol. 124, no. 1274, pp. 447–471, Apr. 2020.

[28] K. Sekine, F. Kato, K. Kageyama, and E. Itoh, "Data-driven simulation for evaluating the impact of lower arrival aircraft separation on available airspace and runway capacity at Tokyo international airport," *Aerospace*, vol. 8, no. 6, p. 165, Jun. 2021.

[29] T. Hirata, A. Shimizu, and T. Yai, "Runway capacity model for multiple crossing runways and impact of tactical sequencing—Case study of Haneda airport in Japan," *Asian Transp. Stud.*, vol. 2, no. 3, pp. 295–308, 2016.

[30] Geospatial Information Authority of Japan. *Maps & Geospatial Information*. Accessed: Apr. 18, 2022. [Online]. Available: https://www.gsi.go.jp/top.html

[31] M. Brown, H. Aoyama, and I. Yamada, "Analysis of Haneda airport spot information for surface movement control," *IEICE Tech. Rep.*, vol. 111, no. 407, pp. 9–14, Jan. 2012. [Online]. Available: https://cir.nii.ac.jp/crid/1520009408558173440

[32] S. Tsuzuki, D. Yanagisawa, and K. Nishinari, "Auto-generation of centerline graphs from geometrically complex roadmaps of real-world traffic systems using hierarchical quadtrees for cellular automata simulations," *Inf. Sci.*, vol. 504, pp. 161–177, Dec. 2019, doi: 10.1016/j.ins.2019.07.049.

[33] D. Martinez, S. Belkoura, S. Cristobal, F. Herrema, and P. Wächter, "A boosted tree framework for runway occupancy and exit prediction," in *Proc. 8th SESAR Innov. Days (SID)*, Salzburg, Austria, 2018.

[34] N. Mirmohammadsadeghi and A. Trani, "Prediction of runway occupancy time and runway exit distance with feedforward neural networks," in *Proc. AIAA Scitech Forum*, Jan. 2020, p. 1402. [Online]. Available: http://arc.aiaa.org

**YOSHIAKI KAWAGOE** received the Ph.D. degree in engineering from Tohoku University, Japan, in 2018. From 2018 to 2020, he was a Specially Appointed Assistant Professor at the Institute of Fluid Science, Tohoku University. Since April 2020, he has been an Assistant Professor with the Department of Aerospace Engineering, Tohoku University. His research interests include multiscale modeling of composite materials for next-generation aircraft and the optimization of surface traffic flow at airports.

**RYOHEI CHINO** received the bachelor's degree in mechanical and aerospace engineering from Tohoku University, Sendai, Japan, in 2022, where he is currently pursuing the master's degree with the Department of Aerospace Engineering, Graduate School. His current research interests include optimization of air traffic flow on airport surfaces and the conceptual design of aircrafts.

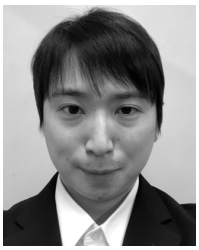

**SATORI TSUZUKI** received the Ph.D. (Dr.Sci.) degree from the Tokyo Institute of Technology, in 2016. He won a Postdoctoral Research Fellowship for young scientists sponsored by the Japan Society for the Promotion of Science (JSPS). He stayed at the Japan Agency for Marine-Earth Science and Technology, from 2016 to 2017. From 2017 to 2020, he worked as a Project Assistant Professor at The University of Tokyo. From 2020 to 2021, he obtained a Postdoctoral Fellowship for research abroad sponsored by JSPS. Since 2021, he has been working as a Project Lecturer at The University of Tokyo. He has won one international award and received nine awards from the authoritative academic associations in Japan.

**ERI ITOH** received the Ph.D. degree in aeronautics and astronautics from The University of Tokyo, Japan, in 2007. After gaining experience at international research organizations, she currently holds the position of an Associate Professor with the Aeronautics and Astronautics Department, The University of Tokyo, and a Chief Researcher with the Air Traffic Management Department, Electronic Navigation Research Institute, National Institute of Maritime, Port and Aviation Technology. Her research interest includes design of automation systems that work with human operators in air traffic management, including airspace and airport operation. Combining data-driven analysis, mathematical models, and simulation studies, she works toward realizing even more efficient and resilient air traffic operations.

**TOMONAGA OKABE** received the Ph.D. degree in engineering from Keio University, Japan, in 1999. He worked as the Director of the Center for Next-Generation Aircrafts, Tohoku University. In 2007, he was a Visiting Associate Professor at Brown University. He has been an Affiliate Professor with the Department of Material Science and Engineering, University of Washington, since 2018. He is currently a Professor at the Department of Aerospace Engineering, Tohoku University. His research interest includes several areas of composite materials, including process modeling, micromechanics, and failure analysis, as well as nanocomposites.